Defects in Mouse Cortical Glutamate Uptake Can Be Unveiled In Vivo by a Two-in-One Quantitative Microdialysis

Sandrine Parrot, Alex Corscadden, Louison Lallemant, Hélène Benyamine, Jean-Christophe Comte, Aline Huguet-Lachon, Geneviève Gourdon, Mário Gomes-Pereira

ACS Chemical Neuroscience

pubs.acs.org/chemneuro Research Article

Defects in Mouse Cortical Glutamate Uptake Can Be Unveiled *In Vivo* by a Two-in-One Quantitative Microdialysis

Sandrine Parrot,* Alex Corscadden, Louison Lallemant, Hélène Benyamine, Jean-Christophe Comte, Aline Huguet-Lachon, Geneviève Gourdon, and Mário Gomes-Pereira

Cite This: *ACS Chem. Neurosci.* 2022, 13, 134−142 Read Online

ACCESS | Metrics & More | Article Recommendations | Supporting Information

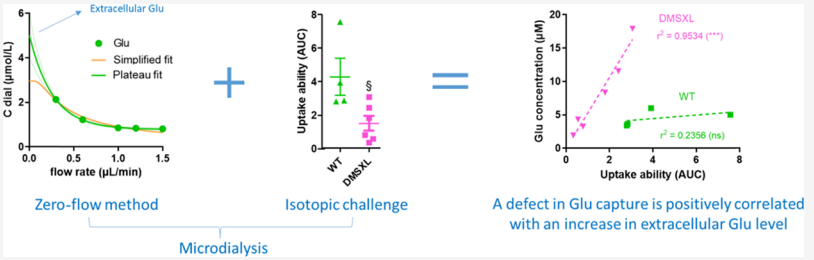

ABSTRACT: Extracellular glutamate levels are maintained low by efficient transporters, whose dysfunction can cause neuronal hyperexcitability, excitotoxicity, and neurological disease. While many methods estimate glutamate uptake *in vitro*/*ex vivo*, a limited number of techniques address glutamate transport *in vivo*. Here, we used *in vivo* microdialysis in a two-in-one approach combining reverse dialysis of isotopic glutamate to measure uptake ability and zero-flow (ZF) methods to quantify extracellular glutamate levels. The complementarity of both techniques is discussed on methodological and anatomical basis. We used a transgenic mouse model of human disease, expressing low levels of the EAAT-2/GLT1 glutamate transporter, to validate our approach in a relevant animal model. As expected, isotopic analysis revealed an overall decrease in glutamate uptake, while the ZF method unveiled higher extracellular glutamate levels in these mice. We propose a sensitive and expedite two-in-one microdialysis approach that is sufficiently robust to reveal significant differences in neurotransmitter uptake and extracellular levels through the analysis of a relatively low number of animals.

KEYWORDS: *glutamate, uptake, motor cortex, quantitative microdialysis, reverse dialysis, in vivo, mouse*

INTRODUCTION

Glutamate (Glu) is the major excitatory neurotransmitter in the central nervous system, and the regulation of its concentration is crucial to maintain normal brain functions. Glu plays many roles in general physiology, such as the regulation of metabolism, cell maturation, and immune response. The variety of targeted receptors, membrane transporters, and modes of Glu release by neurons and astrocytes complicates the study of Glu homeostasis relative to other neurotransmitters. Glu uptake by brain cells is essential to maintain low extracellular levels, prevent hyperexcitability, and avoid neuronal excitotoxicity.[1] Glu uptake relies mainly on five carriers known as excitatory amino acid transporters, including EAAT-1 (SLC1A3 or GLAST), EAAT-3 (SLC1A1 or EAAC-1), EAAT-4 (SLC1A6), or EAAT-5 (SLC1A7). EAAT-2 (SLC1A2 or GLT1) is mainly expressed in astrocytes and contributes to more than 95% of the total uptake activity.[2]

Several *ex vivo* and *in vitro* approaches can estimate Glu uptake, either by measuring messenger RNA (mRNA) and protein levels, which may provide an indirect estimation of the uptake capacity, or by directly evaluating Glu uptake activity. However, quantifying mRNA requires tissue homogenization and denaturation, which abolishes cell organization. *In situ* hybridization allows the detection of RNA splicing isoforms encoding Glu transporters on histological slides with a precise anatomical localization due to the preservation of local cell organization,[3] but it does not assess protein functions. Due to the delay between transcription and translation, mRNA detection is often coupled to protein expression quantification by western blot[4,5] to provide information on post-translational modifications. Fluorescence-activated cell sorting-based methods can quantify glutamate/aspartate transporter (GLAST) and GLT1 in cell cultures;[6] however, this method does not measure functional Glu uptake. Instead, Glu transport activity is usually evaluated in cells or synaptosomes using isotopic aspartate (Asp) or Glu to compete with endogenous Glu.[7]

Received: September 27, 2021
Accepted: December 6, 2021
Published: December 19, 2021

https://doi.org/10.1021/acschemneuro.1c00634
ACS Chem. Neurosci. 2022, 13, 134−142

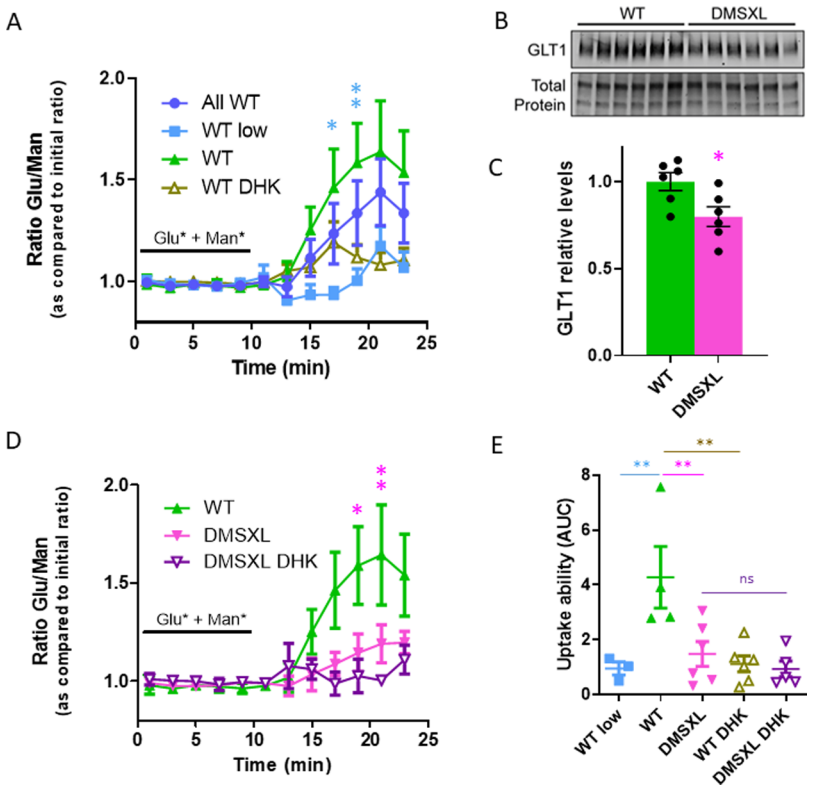

Figure 1. (A) The ability of glutamate uptake was evaluated by comparing the ratio of L-[^{3}H]-Glu/[^{14}C]-Man radioactivity normalized by the ratio of the isotopic solution infused through the microdialysis probe. Data are expressed as mean ± standard error of the mean for "all WT" mice implanted in the motor M1 cortex (n = 7, dark blue circles), including mice with a correct implantation ("WT" mice, n = 4, green triangles) and mice with a low implantation ("WT low" mice; n = 3, fair blue squares). WT mice treated with DHK to challenge our method ("WT DHK" n = 6, olive green triangles) are also presented (ANOVA repeated measures, followed by Bonferroni posthoc tests between "WT" and "WT low" groups, $*p < 0.05$, $**p < 0.01$). (B) Representative western blot detection of GLT1 in the mouse frontal cortex. (C) GLT1 steady-state levels in the frontal cortex of the DMSXL and WT mice at 2 months. Data are means (±SEM, n = 6 per genotype) relative to normalized WT values (two-tailed Student's t-test, $*p < 0.05$). (D) The ability of glutamate uptake in the DMSXL M1 cortex (n = 6, pink triangles) as compared to the WT mice aged 2 months (n = 4, green triangles) and the DMSXL mice in which glutamate uptake was inhibited through the application of DHK (n = 5, purple triangles) was evaluated by comparing the ratio of L-[^{3}H]-Glu/[^{14}C]-Man radioactivity normalized by the ratio of the isotopic solution infused through the microdialysis probe (ANOVA repeated measures, followed by Bonferroni posthoc tests between DMSXL and WT groups, $*p < 0.05$, $**p < 0.01$). (E) Uptake ability of glutamate in the motor cortex is expressed as the AUC of (A,D) (one-way ANOVA test, followed by Šidák's multiple comparison test, $**p < 0.01$).

This approach is not ideal, given the possible variability in the composition of synaptosome preparations (*i.e.*, a greater content in astrocyte membranes is predicted to result in higher Glu uptake).[2] In turn, while cell cultures offer the unique possibility of chemical and genetic manipulation under controlled conditions, they poorly mimic the complexity of the brain structure and the intricate multicellular environment.[2] To overcome these drawbacks, high-speed imaging of an intensity-based Glu-sensing fluorescent reporter (iGluSnFR) coupled to electrophysiological recordings was recently used on brain slices.[8] The results obtained diverged considerably from those obtained using classical Glu challengers, leading to conflicting conclusions. Today, in spite of a variety of approaches being available to study Glu uptake activity, a reliable method to quantify Glu uptake in mice *in vivo* is still needed.

In vivo neurochemical techniques may offer advances and provide better estimations of Glu uptake and extracellular concentration because they take into account the integrity of the targeted brain structure.[7] In line with this view, we propose the use of microdialysis. Microdialysis is a sampling technique that requires the infusion of an artificial cerebrospinal fluid (aCSF) through a probe at a constant flow rate (FR), allowing both diffusion of small endogenous molecules through a concentration gradient and *in situ* drug delivery by reverse dialysis. The isotopic challenge consists in the application, by reverse dialysis, of a mixture of labeled Glu as a transport competitor coupled with labeled mannitol (Man) as a reference molecule.[9,10] This method has been validated in rats, where it confirmed the pharmacological inhibition of Glu uptake by several chemicals, in several brain areas, including the cortex.[7] This approach can be coupled with no-net-flow (NNF) methods for the quantitative microdialysis of endogenous Glu levels.[6,11−13] However, the NNF method has shown some pitfalls: results may display lack of linearity in a nonhomogeneous brain structure (*e.g.*, a complex folded structure like the hippocampus)[7] or as a result of the short length of the dialysis membrane,[14] which can be problematic in animals as small as mice. For these reasons, we decided to assess another quantitative microdialysis method in mice, known as the zero-flow (ZF) method.[15] This method is based on mass transfer according to the FR of aCSF perfusion. The ZF method is easier to carry out than NNF since no exogenous compound is required but relies on nonlinear extrapolation, not linear regressions. However, this technique is usually suitable for peptides or proteins in situations where the NNF

https://doi.org/10.1021/acschemneuro.1c00634
ACS Chem. Neurosci. 2022, 13, 134−142

method is not applicable due to peptide adsorption to the surfaces of the microdialysis setup,[16] but the ZF method has never been used to quantify glutamate. As compared to the NNF method, 2 times fewer samples are required by the ZF method, and the cost of the analysis of Glu content is therefore reduced. Furthermore, in contrast to NNF,[11] the ZF method allows the quantification of several compounds, not only in the same animal but also in the same sample. Another major advantage is that the total duration of the experiment can be reduced to 2 h instead of 6−10 h with a longer sampling time, thanks to the use of capillary electrophoresis or capillary high-performance liquid chromatography as analytical techniques, which display good sensitivity and are compatible with very low-concentration samples.[7] Some experimental bias due to circadian rhythms can also be minimized as well.[7]

For all these reasons, we assessed a dual, quantitative microdialysis approach that combines the measurement of Glu uptake by the administration of labeled Glu, with the quantification of extracellular Glu levels by ZF methods *in vivo*, in the brain of the same mouse. In order to validate our novel two-in-one approach, we applied the microdialysis protocols to a transgenic mouse of human disease displaying abnormal expression of Glu transporters.[17] We demonstrate that the technique is sensitive enough to unveil relevant defects in cortical Glu uptake and abnormal extracellular Glu levels *in vivo* in a mouse that exhibits a ∼20% reduction in GLT1 steady-state levels in frontal cortex. Interestingly, at the individual level, the two-in-one method revealed an intriguing correlation between glutamate uptake and extracellular concentration in these transgenic mice, suggesting defective control of glutamate homeostasis in this condition.

RESULTS AND DISCUSSION

Validation of the Isotopic Approach Used. A solution containing 100 μmol/L ^{3}H-Glu and 120 μmol/L labeled ^{14}C-Man (a compound taken by nonspecific transporters) was chosen to challenge endogenous Glu uptake in mice (Supporting Information, Figure S1). The ratio between ^{3}H-Glu and isotopic ^{14}C-Man, as compared to the initial isotopic Glu/Man ratio, was monitored during and after the application of the labeled compounds. Typical profiles of the isotopic ratios curve are shown in Figures 1A and S2. The ratio between labeled Glu and isotopic Man remained constant during the concomitant application of the two isotopes but varied during the washout period, probably due to the combination of high resistance of the tissue in the mouse brain with low microdialysis recovery (Figures S1 and S2). In the hippocampus, the curves peaked between 4 and 10 min after the end of isotopic infusion, which agrees with the kinetics found in astrocyte cultures,[18] since 95% of glutamate clearance is ensured by an astrocytic carrier.[2] We conclude that under these conditions, our protocol can reproduce *in vivo* uploading of labeled Glu previously reported *in vitro*.

Glu uptake ability was challenged in the frontal cortex of wildtype (WT) mice using exogenous isotopic Glu (Figure 1A). In this brain region, the ratio peaked 12 min on average following isotope perfusion, which is still in accordance with previous data and with a release of Glu after uptake by the cells.[18] In other words, higher release of Glu during washout is suggestive of higher Glu uptake during previous isotopic infusion. This assumption was tested through the pharmacological administration of 2 mmol/L dihydroxykainate (DHK), a Glu uptake inhibitor (Figure 1A). The challenging of the 100 μmol/L labeled Glu infusion with DHK abolished the hump-shaped washout curve, demonstrating that Glu uptake was prevented during the isotopic infusion and that the increase detected during the washout period was essentially due to Glu release following isotopic loading. It is conceivable that washout detection can also represent the release of Glu metabolites, such as glutamine (Gln), resulting from the conversion of exogenous Glu in brain cells.

When considering the experiment without DHK (Figure 1A), we noticed substantial variability in the washout profiles between WT mice. To gain insight into the reasons behind this variability, we used methylene blue dye to determine the anatomical location of the probe in the cortex of individual mice (Figure S3). The analysis revealed a significant correlation between the position of the probe and the Glu/Man washout profiles [analysis of variance (ANOVA) repeated measures, interaction time × implantation, $F(7, 1) = 3.24$, $p = 0.0093$]: the three experiments with deeper probe implantation showed altered Glu/Man ratios when compared to the four experiments with expected probe implantation (Figure 1A,E, "WT low" *vs* "WT" groups). The absent or very low uptake in the "WT low" group likely reflects the lower GLT1 density reported in the deeper cortical layers.[19,20] Therefore, we conclude that isotopic microdialysis yields a robust assessment of Glu uptake in the upper layers of the mouse motor cortex while avoiding the confounding effects of reduced transporter expression in the lower cortical layers.

Validation of the Two-in-One Microdialysis Approach in a Mouse Model of Human Disease. To fully validate the isotopic quantification of Glu uptake in a mouse model of human disease, we studied the DMSXL mice, a transgenic model of myotonic dystrophy type 1 (DM1).[21,22] DM1 is a rare multisystemic disease, mainly characterized by muscle weakness, myotonia, cardiac pathology, as well as cognitive impairment and behavioral changes. DM1 is caused by the expansion of a noncoding trinucleotide CTG repeat in the *DMPK* gene, which results in the expression of toxic RNA transcripts that accumulate in the nucleus. Toxic RNA accumulation deregulates RNA processing in DM1 cells, affecting the expression, activity, and localization of different proteins.[23] The DMSXL transgenic mice carry a large CTG repeat expansion and recreate multisystemic phenotypes, notably in the central nervous system.[24,25] We previously found a significant decrease in GLT1 protein in the DMSXL mouse brain areas involved in motor control and execution, such as the cerebellum and cortex.[17]

We first confirmed GLT1 downregulation in the brain cortex of DMSXL mice studied at 2 months of age (Figure 1B,C). Then, to determine if lower GLT1 levels in the DMSXL cortex resulted in decreased Glu uptake ability, we performed *in vivo* isotopic microdialysis. After verification of the correct placement of the dialysis probe in the upper layers of the motor cortex (Figure S3), we found that the isotopic Glu/Man ratio in DMSXL mice was significantly lower than in WT controls, in agreement with the lower levels of GLT1 [ANOVA repeated measures with $F(7, 1) = 3.93$ as interaction time × genotype, $p = 0.0015$] (Figure 1D). These results indicate altered Glu homeostasis in DMSXL mice in association with a net decrease in Glu uptake. As previously mentioned, we cannot exclude the hypothesis that a fraction of the ^{3}H-labeling recovered at the outlet of the dialysis probe comes not only from labeled Glu, which enters the cells during isotopic loading and is subsequently released during the washout period, but

https://doi.org/10.1021/acschemneuro.1c00634
ACS Chem. Neurosci. 2022, 13, 134−142

also from the intracellular conversion of exogenous Glu into Gln by glutamine ammonia ligase (GLUL), often known as glutamine synthetase (GS). To exclude the contribution of altered Glu conversion in DMSXL mice, we quantified GLUL/GS protein levels in the mouse frontal cortex (Figure S4) and found no differences between the WT and DMSXL mice. These results suggest similar conversion of Glu to Gln in both mouse groups, supporting the idea that the reduced ^{3}H-Glu/^{14}C-Man washout ratio in DMSXL mice reflects fundamentally defective Glu uptake as a result of GLT1 downregulation in these animals. In further support of this conclusion, the administration of DHK resulted in a modest effect in DMSXL mice (Figure 1D), indicative of intrinsically low levels of Glu uptake that are not further decreased by pharmacological inhibition.

ZF Method to Quantify Glu Levels: Fitting Models. We then investigated the consequences of altered uptake ability on the extracellular concentration of Glu *in vivo*. To this end, we used the quantitative ZF microdialysis since it is more suitable for small-sized probes than the alternative NNF.[7] ZF microdialysis is based on the extrapolation of Glu concentrations in the dialysates through the use of regression models. We considered three nonlinear regression models reported in the literature: the theory fit, the simplified fit, and a third model previously used in ZF experiments in humans (Supporting Information, Table S1). Given the poor fitting of the published models to our experimental results (Tables S2 and S3, Figure 2), we tested a new regression model: the

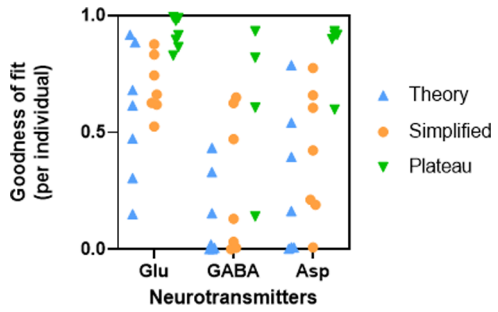

Figure 2. Individual goodness of fit for each fit model tested *in vivo* to quantify Glu, GABA, and Asp levels in seven WT mice. Some values of r^2 are missing for GABA and Asp using plateau fit (see Tables S2–S4 and text in the Supporting Information for further details).

plateau fit. In contrast to dopamine, the monoamine neurotransmitter for which the theory and simplified models were previously validated and whose concentration approaches zero with increasing FRs,[26] Glu levels show a different profile. The new plateau fit tested takes into account the experimental observation that the dialysate concentration of Glu trended to a value different from zero when very high FRs were used.

The plateau model takes into consideration not only the experimental profile of the Glu ZF data but also the weight of the multiple sources of Glu release in the brain (neurons and non-neuronal cells) and the numerous proteins regulating its basal levels.[7] It is well documented that the origin of extracellular Glu is mainly non-neuronal since it is not sensitive to means of preventing neuronal release (tetrodotoxin or low concentration of extracellular calcium) in contrast to dopamine, for instance.[27] Importantly, the plateau model is likely suited to fit gamma-aminobutyric acid (GABA) and Asp as well (Figure 2), whose ZF levels exhibited a profile similar to Glu. In support of a shared plateau model between these neurotransmitters, it is worth noting that GABA and Asp levels and metabolism are strongly linked to Glu: GABA derives from Glu, while Asp and Glu share the same uptake transporter. For all these reasons, we introduced a lower plateau of Glu concentration in our regression "plateau model": $C_{dial} = (C_{ext} - \text{plateau}) \times \exp^{-KX} + \text{plateau}$, where C_{dial} is the dialysate concentration of Glu at the FR (here, the parameter X), C_{ext} is the true concentration of extracellular Glu, X is the FR, and plateau and K are constant values. The plateau model exhibited the best fitting to our ZF curves as compared to the two other models tested (Figures 2 and S5; Table S4 *vs* S2 and S3; statistical analyses and the interpretation of the comparisons are available in the Supporting Information). However, the plateau model sometimes fails in cases of very low concentrations of Asp and GABA when the bioavailability of these neurotransmitters in the brain structure is limited (Figure S6).

To corroborate the importance of considering the *in vivo* ZF profile of a neurotransmitter amino acid and to validate our "plateau fit" model as a suitable method to quantify extracellular Glu, we tested how well the model predicts Glu concentration in standard solutions *in vitro*. Similar C_{ext} values were found using the three models, but they were nonetheless lower than the theoretical Glu concentrations (Figure S7), showing that they all underestimated the levels of this neurotransmitter. More importantly, our results clearly demonstrate that through the introduction of a new and versatile parameter, the plateau model is a relevant alternative to the classical fitting models, allowing the precise extrapolation of true extracellular Glu concentrations *in vitro* with a modest improvement in accuracy as compared to the classical ZF models tested.

We then applied the three models to ZF data collected *in vivo* in WT and DMSXL mice to determine the extracellular levels of Glu in these animals [Figure 3 (top) for the ZF values, Table S5]. Since Glu uptake is significantly reduced in the DMSXL mouse cortex, we expected an increase in extracellular Glu levels, as previously reported in a rodent model of epilepsy.[11] We also measured the extracellular levels of Asp [an amino acid also transported by GLT1, Figure 3 (middle)] and GABA [a neurotransmitter taken by different transporters, Figure 3 (bottom)] as positive and negative control compounds, respectively. Interestingly, we found some differences in the degree of variability of the C_{ext} calculated and in their confidence intervals inferred by the different methods (Figure 3; Table S5). Overall, the usual simplified fitting resulted in lower variability of neurotransmitter concentrations in both genotypes and revealed one outlier in DMSXL mice (Grubbs' test, $p < 0.05$; see the outlier kept and displayed in Figure 3). The variability in Glu and Asp levels inferred by the theory and plateau fitting was significantly higher in the DMSXL mice than in the WT controls (F test included in Welch's test to compare both variance and mean, $p < 0.05$) without revealing any significant outlier (Grubb's test, $p < 0.05$). Moreover, we found that the theory fit underestimated GABA levels when compared to the other regression methods.

From the careful comparison between models, we conclude that the choice of regression fitting has a pronounced impact on the evaluation of neurotransmitter concentrations *in vivo* by ZF microdialysis. No previous studies have provided a critical parallel of the different regression models, nor have they investigated the concentrations of multiple neurotransmitters

https://doi.org/10.1021/acschemneuro.1c00634
ACS Chem. Neurosci. 2022, 13, 134−142

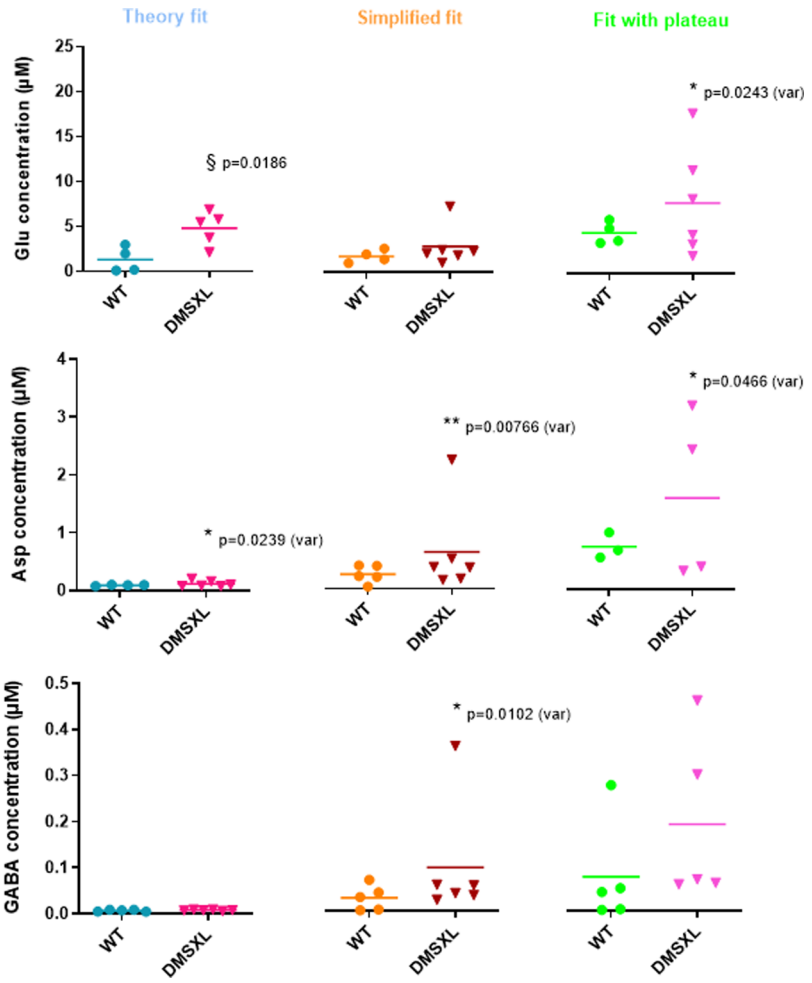

Figure 3. Extracellular levels of Glu (top), Asp (middle), and GABA (bottom) determined in the cortex of 2 month-old WT and DMSXL mice using the theory, simplified, and plateau fit. DMSXL mice showed significantly higher Glu levels when the theory fit was applied (two-tailed Student's *t*-test, $^{\S}p < 0.05$), as well as higher variances of Glu, Asp, and GABA levels (Student's *t*-test with Welch's correction, $^{*}p < 0.05$; $^{**}p < 0.01$).

in two different subject groups. Overall, our data demonstrate the benefits of incorporating a minimal plateau in nonlinear extrapolation models to improve their fitting.

Correlation between Neurotransmitter Uptake and Extracellular Concentration in Individual Mice. After measuring Glu uptake ability and Glu extracellular concentrations, we sought to investigate the correlation between both measurements in individual animals. In other words, we asked if the individual levels of extracellular Glu correlated inversely with Glu uptake within each mouse group. To address this question, we calculated the area under the curve (AUC) of the Glu/Man ratio measured after the isotopic challenge (*i.e.*, from $t = 10$ min to $t = 26$ min) for each mouse (Figure 1E) and used it as an estimate of the uptake ability in the WT and DMSXL mice (Figure 4A). Overall, and in line with the downregulation of GLT1, the average AUC was significantly lower in the frontal cortex of the DMSXL mice relative to the WT controls, corroborating defective Glu uptake in transgenic DM1 mice.

We then investigated how AUC values correlated with the extracellular levels of Glu, Asp, and GABA in individual mice. The variability in Glu uptake ability among WT animals did not correlate significantly with the levels of Glu (Figure 4B), regardless of the regression model used to extrapolate the extracellular concentration of this neurotransmitter. It is conceivable that the complex and efficient regulation of Glu homeostasis by different proteins and transporters[7] ensures strict control of the extracellular Glu levels in the WT mice. Independently of its cellular origin, Glu must be tightly regulated and avoid fluctuations that may result in altered neuronal activity. Similarly, Asp (Figure 4C) and GABA (Figure 4D) levels did not correlate with Glu uptake. We then extended our analysis to DM1 transgenic mice with defective GLT1 expression to further validate our *in vivo* quantitative microdialysis and assess Glu homeostasis in these animals. In contrast with the WT controls, the DMSXL mice displayed a surprisingly positive correlation between Glu uptake and the extracellular levels of Glu and Asp, extrapolated by the plateau fitting model (Figure 4B,C): higher ability to uptake Glu was associated with higher concentrations of both compounds in the brain motor cortex. This intriguing result may be the consequence of the deregulation of Glu homeostasis in DM1 mice and the dysfunction of the associated mechanisms that promote Glu transport in response to excessive extracellular concentration. In contrast to Glu and Asp, GABA did not show a significant correlation with Glu uptake ability in DMSXL mice (Figure 4D), demonstrating the specificity of the Glu transporter system to the former compounds. We are currently

https://doi.org/10.1021/acschemneuro.1c00634
ACS Chem. Neurosci. 2022, 13, 134−142

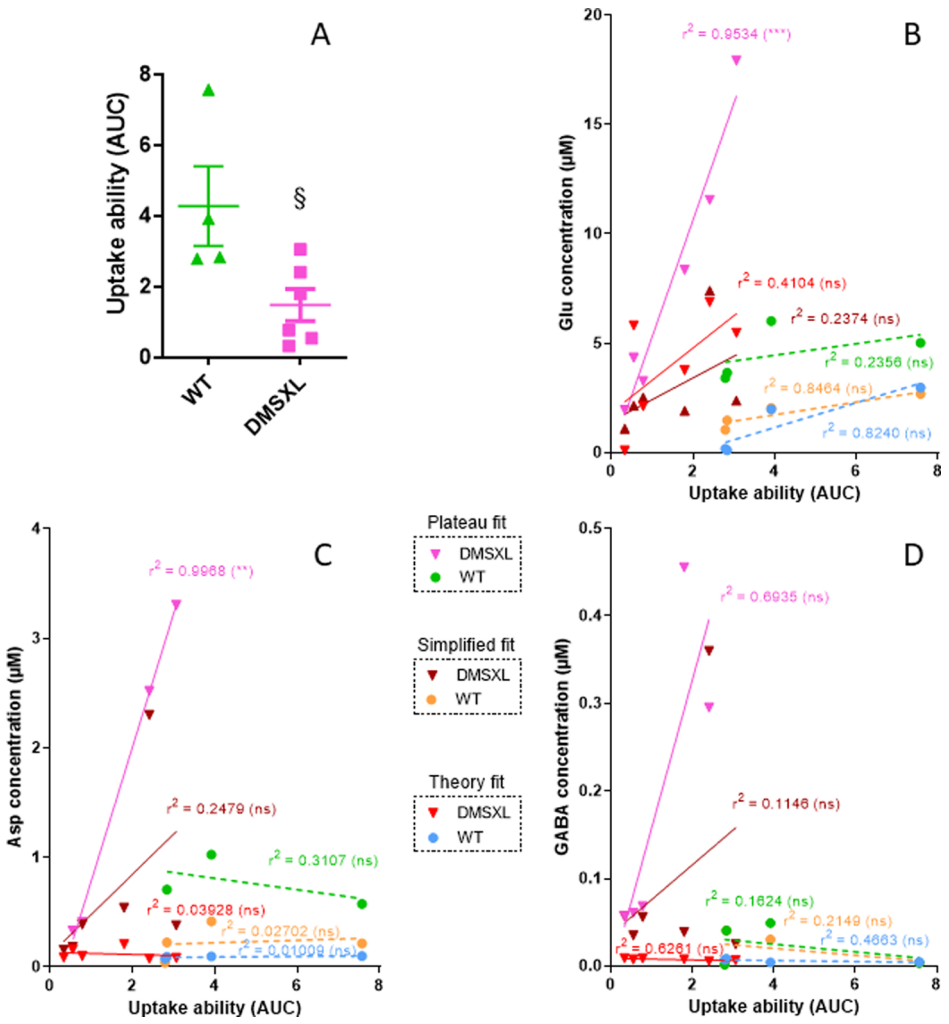

Figure 4. (A) Uptake ability of Glu in the motor cortex (already shown in Figure 1E) is expressed as the AUC of Figure 1A,D (two-tailed Student's *t*-test, $^{\S}p = 0.0295$). Uptake ability is compared to the extracellular levels of Glu (B), Asp (C), and GABA (D) determined in the cortex of the WT and DMSXL mice using three models of fitting in ZF experiments: theory, simplified, and plateau fit (Pearson *r* test, $^{***}p = 0.008$ for Glu, and $^{**}p = 0.002$ for Asp).

investigating the underlying mechanisms that explain these observations in the DMSXL mice.

Final Remarks. We coupled two quantitative *in vivo* methods to determine Glu uptake ability and Glu levels in the cortex of mice through isotopic challenge and ZF microdialysis, respectively. The two-in-one approach combining quantitative microdialysis and isotopic challenge has been previously used and validated in rats to study the impact of defective Glu transport *in vivo*.[6,7,11] One advantage of the isotopic approach is that as few as 4−6 animals are sufficient to detect significant alterations in uptake capacity *in vivo*. In addition, only a 10 min perfusion is necessary for the administration the isotopic solution so that the total sampling (including a baseline determination and the washout period) does not exceed 30 min. Therefore, the isotopic approach can be coupled with a concomitant experiment for the determination of extracellular Glu levels in the same animal, in full accordance with the ethical guidelines that encourage the reduction of the number of animals used for scientific purposes. The concomitant ZF microdialysis and analysis of the isotopic loss at the outlet of the probe after a quantitative perfusion of labeled Glu provides a powerful approach to investigate brain neurochemistry *in vivo* and determine both Glu extracellular concentrations and Glu uptake ability. We developed a new two-in-one approach that allows careful comparison of both parameters between mouse groups and that is capable of unraveling novel correlations within individual mouse groups. The introduction of a lower plateau in the original one-decay ZF regression not only takes into account biological features of the experimental profiles collected but it also provides an improvement to extrapolate extracellular Glu concentrations *in vivo* from ZF data. The risks associated with nonlinear extrapolation were considered and minimized by the use of powerful statistical tools. Importantly, we validated the combined quantitative microdialysis approaches in a mouse model of human disease that expresses low levels of Glu transporters, confirming reduced Glu uptake and altered Glu homeostasis in the mouse motor cortex. The two-in-one microdialysis approach that we propose can thus reveal significant differences in relevant mouse models of neurological disease and help decipher the underlying mechanisms.

METHODS

Animals. DMSXL transgenic mice (>99% C57BL/6 background) carrying 45 kb of human genomic DNA from a DM1 patient with

https://doi.org/10.1021/acschemneuro.1c00634
ACS Chem. Neurosci. 2022, 13, 134−142

more than 1500 CTG repeats[21,22] were studied at 2 months of age. The DMSXL status was assessed by multiplex PCR, as previously described.[25] Our study was carried out according to the current European Communities Council Directives (EU Directive 2010/63/EU for animal experiments). The mice were bred and nursed at CERFE Genopole (Evry, France) before being sent to our labs at ∼1.5 months of age. They were acclimated to their new environment and cared for attentively for at least 7 days prior to the study with food and water ad libitum. The housing temperature was kept constant (21 ± 1 °C), and the light/dark cycle was 12 h/12 h, with light beginning at 7:00 a.m. All the mice were studied at 2 months of age. A first group of six WT and six DMSXL mice were used to perform protein blotting and GLT1 immunodetection, and quantification was performed as previously described.[17] A second pool of mice, six WT and six DMSXL, were used to quantify GLUL, also known as GS. A third pool of mice were used in *in vivo* microdialysis experiments (details given in the section "In Vivo Microdialysis Study").

Western Blot Analysis. Protein blotting and GLT1 immunodetection and quantification were performed as previously described.[17] GLUL, known as GS, was also detected and quantified. In brief, the total protein was extracted from 20 to 30 mg of brain tissue dissected from 2 month-old mice, using radioimmunoprecipitation assay buffer (Thermo Fisher Scientific, 89901), supplemented with 0.05% CHAPS (Sigma, C3023), 1× complete protease inhibitors (Roche, 04693124001), and 1× Phospho STOP phosphatase inhibitors (Roche, 04693124001). Protein concentrations were determined using the Pierce BCA protein assay kit (Thermo Scientific, 23227). The total protein (5 μg for GLUL immunodetection and 40 μg for GLT1 immunodetection) was mixed with 4× Laemmli sample buffer (Bio-Rad, 1610747), denatured for 5 min at 95 °C, and resolved in 10% TGX stain-free polyacrylamide gels (Bio-Rad, 1610183). After electrophoresis, the gels were activated for 45 s under UV light, proteins were transferred onto nitrocellulose membranes using a Trans-Blot transfer system (Bio-Rad), and total protein on the membrane was imaged using the ChemiDoc imaging system (Bio-Rad). The membranes were then blocked in 5% Blotto nonfat dry milk (Santa Cruz Biotech, sc2325) in 1× TBS-T (10 mM Tris-HCl, 0.15 M NaCl, and 0.05% Tween 20) for 1 h at room temperature (RT) and incubated with the primary antibody overnight at 4 °C: anti-GLT1 (gift from Dr. Jeffrey Rothstein, Johns Hopkins, USA; 1:5000 dilution), anti-GLUL (GeneTex, GTX109121; 1:20,000 dilution), and antitubulin (Sigma, T4026; 1:2000 dilution). After three washes in 1× TBS-T, the membranes were incubated with IRDye 800CW donkey antirabbit (LI-COR Biosciences, P/N 926-32213) for 1 h at RT and washed three times. Antibody binding was visualized by fluorescence using an LI-COR Odyssey CLx imaging system. Densitometric analysis was performed using Image Studio Lite software. The normalized protein expression levels were expressed relative to the average of control samples.

***In Vivo* Microdialysis Study.** Out of the 28 mice initially scheduled, 3 mice died before the end of experiment while being anaesthetized and their data were either absent or incomplete; one WT mouse gave atypical data and was excluded; one DMSXL mouse was excluded due to an inaccurate implantation; hence, the data of 13 WT mice (weighing 22.2 ± 2.9 g, aged 61 ± 5 days) and 11 DMSXL mice (weighting 16.0 ± 1.6 g, aged 64 ± 5 days) were finally included in our microdialysis experiments. The mice were anaesthetized with a mixture of medetomidine chlorhydrate (1 mg/kg)/ketamine (75 mg/kg), and anesthesia was maintained for 5 h with ketamine: at t + 1 h and t + 2 h for 1/2-dose and at t + 3 h and t + 4 h for 1/4-dose. The body temperature was maintained constant using a heating pad. Once deep anesthesia was verified through the absence of hind paw withdrawal after pinching, the mouse was placed in a stereotaxic frame (David Kopf), the skin was incised, and the skull was cleaned and exposed. A hole was drilled, and the meninges were resected to allow the implantation of the single-use homemade dialysis probe (MWCO 6000 Da, 1 mm active membrane, 225 mm o.d., infused at 1 μL/min) in the right motor M1 cortex at the following coordinates related to bregma: AP +2 mm, ML 1.8 mm, DV −1 mm from the dura for WT mice.[28] The ML coordinates were slightly adapted to 1.6 mm for the DMSXL mice, given their small size. After 1 h 30 min post-implantation, the FR was increased to 1.5 μL/min to initiate ZF experiments at 1 h 45 min postimplantation. In brief, aCSF (149 mmol/L NaCl, 2.80 mmol/L KCl, 1.2 mmol/L $MgCl_2$, 1.2 mmol/L $CaCl_2$, 2.78 mmol/L phosphate buffer, pH 7.4, made with sterile ultrapure water and 0.22 μm-filtered) was perfused at five successive FRs (1.5, 1.2, 1, 0.6, and 0.3 μL/min) as follows: 5 min stabilization time (except 10 min for 0.3 μL/min, allowing a flush considering the dead volume between the dialysis membrane and the outlet of the probe, *i.e.*, 0.5 μL)[29] followed by a sampling time (2, 2.5, 3, 5, and 10 min), allowing the collection of 3 μL samples in triplicate. Then, the FR was reinitiated to 1 μL/min for the second part of the experiment. After the collection of three 2 min samples, a solution of 100 μmol/L ^{3}H-Glu (49.7 Ci/mmol) and 120 μmol/L ^{14}C-Man (57.2 mCi/mmol) (PerkinElmer) was infused in the probe for 10 min while collecting five other samples. Normal aCSF perfusion was then restored for the collection of last seven samples during that washout period. The samples were collected in sterile PCR tubes and stored at −30 °C until capillary electrophoresis with laser-induced fluorescence detection (CE-LIFD) analysis and at −20 °C until isotopic quantification. At the end of the experiment, methylene blue (0.1%) was perfused to tag the membrane tract. The mice were then euthanized with a lethal dose of pentobarbital immediately after the removal of the probe. The brains were removed and then, while being exposed in a flat position, coronally sectioned at the level of the tract, using a scalpel maintained vertically. This freehand cutting avoids disseminating radioactive isotopes that would occur in a cryostat on a frozen brain. A photograph of the brain section is compared to the stereotaxic atlas (Figure S3).[28] Indeed, although ZF experiments are carried out on the same animal as the isotopic challenge, they must be performed before the application of the isotopic solution to avoid disseminating traces of radioactivity in the samples analyzed by an analytical device, which is not designed to operate on isotopes.

Neurotransmitter Amino Acid Analysis. Glu, Asp, and GABA levels in the ZF dialysates were determined using CE-LIFD as follows: on the day of analysis, 3 μL of the sample and 3 μL of the standard solutions were derivatized at RT by adding 1.2 μL of a mixture (1:2:1 v/v/v) of (i) the internal standard (100 μmol/L cysteic acid in 0.117 mol/L perchloric acid), (ii) a borate/NaCN solution (100:20 v/v mixture of 500 mmol/L borate buffer, pH 8.7, and 87 mmol/L NaCN in water), and (iii) a 2.925 mmol/L solution of naphthalene-2,3-dicarboxaldehyde in acetonitrile/water (50:50 v/v). The samples were then analyzed using an automatic capillary zone electrophoresis P/ACE MDQ system (Beckman, USA) equipped with a ZETALIF laser-induced fluorescence detector (Picometrics, France). Excitation was performed using a 410 nm diode laser (Melles Griot, USA). Separations were carried out on a 63 cm × 50 μm i.d. fused-silica capillary (Composite Metal Services, Worcester, England) with an effective length of 52 cm. The capillary was sequentially flushed with 0.25 mol/L NaOH (15 min), ultrapure water (15 min), and running buffer (75 mmol/L sodium borate, pH 9.20 ± 0.02, containing 10 mmol/L HP-β-CD and 70 mmol/L sodium dodecyl sulfate) (5 min) daily prior to the analysis. The separation was carried out with an applied voltage of 25 kV, hydrodynamic sample injection (10 s at 0.6 psi), and a temperature between 30 and 38 °C. The capillary was sequentially flushed for 30 s each with 0.25 mol/L NaOH, ultrapure water, and running buffer between analyses. Electropherograms were acquired at 15 Hz using P/ACE MDQ software.[30] The concentrations of each amino acid analyte in the dialysate samples (C_{out}) obtained during perfusion under various FRs were used to construct an exponential regression plot of either $C_{out} = C_{ext}(1 - \exp^{-K/FR})$ (called "theory fit" or model 1), $C_{out} = C_{ext} \times \exp^{-K \times FR}$ (called simplified, usual fit, or model 2), or $C_{out} = (C_{ext} - \text{plateau}) \times \exp^{-K \times FR} + \text{plateau}$ (called plateau fit or model 4), where C_{ext} is the true extracellular concentration when the FR is zero and K and plateau are constant values. Curve adjustments for theory fit were performed using MATLAB software. Curve adjustments for simplified and plateau fits and all other statistical analyses were performed using GraphPad Prism (version 5) software, including an automatic outlier

https://doi.org/10.1021/acschemneuro.1c00634
ACS Chem. Neurosci. 2022, 13, 134−142

elimination. ANOVA was not relevant for a global analysis due to the heteroscedasticity of the data obtained using the fittings.

Isotopic Quantification. For radioactivity experiments, on the day of counting, caps of the PCR collection tubes were opened, and the tubes were placed in counting vials with 150 μL of ultrapure water and 2.5 mL of Ultima Gold universal liquid scintillation cocktail. Once stirred and kept in the dark for least 2 h in the counter, the dual counting started (10 min par sample, TRI-CARB 4910TR, PerkinElmer). The ratio of disintegrations per minute between Glu and Man was calculated and normalized by the initial ratio of the isotopic solution. A change in this ratio during the isotopic experiment was evidenced using ANOVA with repeated measures, followed by a Bonferroni posthoc test. An AUC analysis was also included for the seven points of the curve after the isotopic challenge with ^{3}H-Glu and ^{14}C-Man. The analyses and comparisons were done using GraphPad Prism (version 5) software.

***In Vitro* Microdialysis Study.** Five dialysis probes were used twice to compare the three fittings of theory, simplified, and plateau models. The ZF method was carried out *in vitro* in a 10 μM Glu solution containing 0.1, 1, or 10 μM ^{3}H-Glu (three or four assays per concentration, n = 10 in total). The Glu content was quantified with the Ultima Gold universal liquid scintillation cocktail and simple counting. Curve adjustments for theory fit were performed using MATLAB software. Curve adjustments for simplified and plateau fits and all other statistical analyses were performed using GraphPad Prism (version 5) software.

■ ASSOCIATED CONTENT

Supporting Information

The Supporting Information is available free of charge at https://pubs.acs.org/doi/10.1021/acschemneuro.1c00634.

Glu uptake: methodological parameters to be considered, verification of probe placement, and quantification of GS (EC 6.3.1.2), ZF fitting models: *in vivo* study, and ZF fitting models: *in vitro* study (PDF)

MATLAB main script (PDF)

Associated MATLAB script 1 (PDF)

Associated MATLAB script 2 (PDF)

Associated MATLAB script 3 (PDF)

■ AUTHOR INFORMATION

Corresponding Author

Sandrine Parrot − *Inserm U1028, CNRS UMR5292, Université de Lyon, Lyon Neuroscience Research Center, Bron F-69500, France;* orcid.org/0000-0002-9836-0391; Phone: +33 4 81 10 65 86; Email: sandrine.parrot@univ-lyon1.fr

Authors

Alex Corscadden − *Inserm U1028, CNRS UMR5292, Université de Lyon, Lyon Neuroscience Research Center, Bron F-69500, France*

Louison Lallemant − *Sorbonne Université, Inserm, Institut de Myologie, Centre de Recherche en Myologie, Paris 75013, France*

Hélène Benyamine − *Sorbonne Université, Inserm, Institut de Myologie, Centre de Recherche en Myologie, Paris 75013, France*

Jean-Christophe Comte − *Inserm U1028, CNRS UMR5292, Université de Lyon, Lyon Neuroscience Research Center, Bron F-69500, France*

Aline Huguet-Lachon − *Sorbonne Université, Inserm, Institut de Myologie, Centre de Recherche en Myologie, Paris 75013, France*

Geneviève Gourdon − *Sorbonne Université, Inserm, Institut de Myologie, Centre de Recherche en Myologie, Paris 75013, France*

Mário Gomes-Pereira − *Sorbonne Université, Inserm, Institut de Myologie, Centre de Recherche en Myologie, Paris 75013, France*

Complete contact information is available at: https://pubs.acs.org/10.1021/acschemneuro.1c00634

Author Contributions

Design of the experiments: S.P. and M.G.-P. Experiments and data collection: S.P., A.C., L.L., H.B., and A.H.-L. Data analysis: S.P., A.C., L.L., H.B., and J.-C.C. Writing of the paper: S.P., A.C., G.G., and M.G.-P.

Funding

This work was supported by AFM-Téléthon (AFM project #19920), the Fondation pour la Recherche Médicale (grant number PLP201910009933, to L.L.), the Institut National de la Santé et de la Recherche Médicale (INSERM), the Centre National de la Recherche Scientifique (CNRS), and the Université Claude Bernard Lyon 1 and Paris Ile-de-France Region.

Notes

The authors declare no competing financial interest.

■ ACKNOWLEDGMENTS

We thank Dr. Jeffrey Rothstein for providing the anti-GLT1 antibody. We thank Ombeline Jeannerod for her technical help with the *in vitro* experiments. The authors are also grateful to the personnel of Centre d'Exploration et de Recherche Fonctionelle Expérimentale (CERFE, Genopole, Evry, France) and the animal facility of Lyon Neuroscience Research Center for attentively caring for the mice, especially Jean-Luc Charieau who left us prematurely.

■ REFERENCES

(1) Rothstein, J. D.; Dykes-Hoberg, M.; Pardo, C. A.; Bristol, L. A.; Jin, L.; Kuncl, R. W.; Kanai, Y.; Hediger, M. A.; Wang, Y.; Schielke, J. P.; Welty, D. F. Knockout of glutamate transporters reveals a major role for astroglial transport in excitotoxicity and clearance of glutamate. *Neuron* **1996**, *16*, 675−686.

(2) Danbolt, N. C.; Furness, D. N.; Zhou, Y. Neuronal vs glial glutamate uptake: Resolving the conundrum. *Neurochem. Int.* **2016**, *98*, 29−45.

(3) Münch, C.; Ebstein, M.; Seefried, U.; Zhu, B.; Stamm, S.; Landwehrmeyer, G. B.; Ludolph, A. C.; Schwalenstöcker, B.; Meyer, T. Alternative splicing of the 5′-sequences of the mouse EAAT2 glutamate transporter and expression in a transgenic model for amyotrophic lateral sclerosis. *J. Neurochem.* **2002**, *82*, 594−603.

(4) Dutuit, M.; Touret, M.; Szymocha, R.; Nehlig, A.; Belin, M.-F.; Didier-Bazes, M. Decreased expression of glutamate transporters in genetic absence epilepsy rats before seizure occurrence. *J. Neurochem.* **2002**, *80*, 1029−1038.

(5) Behrens, P. F.; Franz, P.; Woodman, B.; Lindenberg, K. S.; Landwehrmeyer, G. B. Impaired glutamate transport and glutamate-glutamine cycling: downstream effects of the Huntington mutation. *Brain* **2002**, *125*, 1908−1922.

(6) Marignier, R.; Ruiz, A.; Cavagna, S.; Nicole, A.; Watrin, C.; Touret, M.; Parrot, S.; Malleret, G.; Peyron, C.; Benetollo, C.; Auvergnon, N.; Vukusic, S.; Giraudon, P. Neuromyelitis optica study model based on chronic infusion of autoantibodies in rat cerebrospinal fluid. *J. Neuroinflammation* **2016**, *13*, 111.

(7) Parrot, S.; Touret, M.; Denoroy, L. In vivo determination of glutamate uptake by brain microdialysis. In *Biochemical Approaches for*

Glutamatergic Neurotransmission; Parrot, S., Denoroy, L., Eds.; Springer, 2018; pp 431−467.
(8) Parsons, M. P.; Vanni, M. P.; Woodard, C. L.; Kang, R.; Murphy, T. H.; Raymond, L. A. Real-time imaging of glutamate clearance reveals normal striatal uptake in Huntington disease mouse models. *Nat. Commun.* **2016**, *7*, 11251.
(9) Bruhn, T.; Christensen, T.; Diemer, N. H. Microdialysis as a tool for in vivo investigation of glutamate transport capacity in rat brain. *J. Neurosci. Methods* **1995**, *59*, 169−174.
(10) Alexander, G. M.; Grothusen, J. R.; Gordon, S. W.; Schwartzman, R. J. Intracerebral microdialysis study of glutamate reuptake in awake, behaving rats. *Brain Res.* **1997**, *766*, 1−10.
(11) Touret, M.; Parrot, S.; Denoroy, L.; Belin, M.-F.; Didier-Bazes, M. Glutamatergic alterations in the cortex of genetic absence epilepsy rats. *BMC Neurosci.* **2007**, *8*, 69.
(12) Lonnroth, P.; Jansson, P. A.; Smith, U. A microdialysis method allowing characterization of intercellular water space in humans. *Am. J. Physiol.* **1987**, *253*, E228−E231.
(13) Parsons, L. H.; Justice, J. B., Jr. Quantitative approaches to in vivo brain microdialysis. *Crit. Rev. Neurobiol.* **1994**, *8*, 189−220.
(14) Chen, K. C. Insensitivity of the microdialysis zero-net-flux method to nonlinear uptake and release processes. *Neurosci. Res.* **2003**, *46*, 251−256.
(15) Jacobson, I.; Sandberg, M.; Hamberger, A. Mass transfer in brain dialysis devices–a new method for the estimation of extracellular amino acids concentration. *J. Neurosci. Methods* **1985**, *15*, 263−268.
(16) Ulrich, J. D.; Burchett, J. M.; Restivo, J. L.; Schuler, D. R.; Verghese, P. B.; Mahan, T. E.; Landreth, G. E.; Castellano, J. M.; Jiang, H.; Cirrito, J. R.; Holtzman, D. M. In vivo measurement of apolipoprotein E from the brain interstitial fluid using microdialysis. *Mol. Neurodegener.* **2013**, *8*, 13.
(17) Sicot, G.; Servais, L.; Dinca, D. M.; Leroy, A.; Prigogine, C.; Medja, F.; Braz, S. O.; Huguet-Lachon, A.; Chhuon, C.; Nicole, A.; Gueriba, N.; Oliveira, R.; Dan, B.; Furling, D.; Swanson, M. S.; Guerrera, I. C.; Cheron, G.; Gourdon, G.; Gomes-Pereira, M. Downregulation of the Glial GLT1 Glutamate Transporter and Purkinje Cell Dysfunction in a Mouse Model of Myotonic Dystrophy. *Cell Rep.* **2017**, *19*, 2718−2729.
(18) Parpura, V.; Liu, F.; Brethorst, S.; Jeftinija, K.; Jeftinija, S.; Haydon, P. G. Alpha-latrotoxin stimulates glutamate release from cortical astrocytes in cell culture. *FEBS Lett.* **1995**, *360*, 266−270.
(19) Sutherland, M.; Delaney, T.; Noebels, J. Glutamate transporter mRNA expression in proliferative zones of the developing and adult murine CNS. *J. Neurosci.* **1996**, *16*, 2191−2207.
(20) Milton, I. D.; Banner, S. J.; Ince, P. G.; Piggott, N. H.; Fray, A. E.; Thatcher, N.; Horne, C. H. W.; Shaw, P. J. Expression of the glial glutamate transporter EAAT2 in the human CNS: an immunohistochemical study. *Brain Res. Mol. Brain Res.* **1997**, *52*, 17−31.
(21) Seznec, H.; Lia-Baldini, A. S.; Duros, C.; Fouquet, C.; Lacroix, C.; Hofmann-Radvanyi, H.; Junien, C.; Gourdon, G. Transgenic mice carrying large human genomic sequences with expanded CTG repeat mimic closely the DM CTG repeat intergenerational and somatic instability. *Hum. Mol. Genet.* **2000**, *9*, 1185−1194.
(22) Gomes-Pereira, M.; Foiry, L.; Nicole, A.; Huguet, A.; Junien, C.; Munnich, A.; Gourdon, G. CTG trinucleotide repeat "big jumps": large expansions, small mice. *PLoS Genet.* **2007**, *3*, No. e52.
(23) Braz, S. O.; Acquaire, J.; Gourdon, G.; Gomes-Pereira, M. Of Mice and Men: Advances in the Understanding of Neuromuscular Aspects of Myotonic Dystrophy. *Front. Neurol.* **2018**, *9*, 519.
(24) Huguet, A.; Medja, F.; Nicole, A.; Vignaud, A.; Guiraud-Dogan, C.; Ferry, A.; Decostre, V.; Hogrel, J.-Y.; Metzger, F.; Hoeflich, A.; Baraibar, M.; Gomes-Pereira, M.; Puymirat, J.; Bassez, G.; Furling, D.; Munnich, A.; Gourdon, G. Molecular, physiological, and motor performance defects in DMSXL mice carrying >1,000 CTG repeats from the human DM1 locus. *PLoS Genet.* **2012**, *8*, No. e1003043.
(25) Hernández-Hernández, O.; Guiraud-Dogan, C.; Sicot, G.; Huguet, A.; Luilier, S.; Steidl, E.; Saenger, S.; Marciniak, E.; Obriot, H.; Chevarin, C.; Nicole, A.; Revillod, L.; Charizanis, K.; Lee, K.-Y.; Suzuki, Y.; Kimura, T.; Matsuura, T.; Cisneros, B.; Swanson, M. S.; Trovero, F.; Buisson, B.; Bizot, J.-C.; Hamon, M.; Humez, S.; Bassez, G.; Metzger, F.; Buée, L.; Munnich, A.; Sergeant, N.; Gourdon, G.; Gomes-Pereira, M. Myotonic dystrophy CTG expansion affects synaptic vesicle proteins, neurotransmission and mouse behaviour. *Brain* **2013**, *136*, 957−970.
(26) Chen, K. C. Validity of intracerebral microdialysis. In *Handbook of Microdialysis Methods, Applications and Perspectives*; Westerink, B. H. C., Cremers, T. I. F. H., Eds.; Elsevier, 2006; pp 47−70.
(27) Timmerman, W.; Westerink, B. H. C. Brain microdialysis of GABA and glutamate: what does it signify? *Synapse* **1997**, *27*, 242−261.
(28) Franklin, K.; Paxinos, G. *The Mouse Brain in Streotaxic Coordinates*; Academic Press, 2001.
(29) Parrot, S.; Bert, L.; Renaud, B.; Denoroy, L. Glutamate and aspartate do not exhibit the same changes in their extracellular concentrations in the rat striatum after N-methyl-D-aspartate local administration. *J. Neurosci. Res.* **2003**, *71*, 445−454.
(30) Sauvinet, V.; Parrot, S.; Benturquia, N.; Bravo-Moratón, E.; Renaud, B.; Denoroy, L. In vivo simultaneous monitoring of gamma-aminobutyric acid, glutamate, and L-aspartate using brain microdialysis and capillary electrophoresis with laser-induced fluorescence detection: Analytical developments and in vitro/in vivo validations. *Electrophoresis* **2003**, *24*, 3187−3196.

https://doi.org/10.1021/acschemneuro.1c00634
ACS Chem. Neurosci. 2022, 13, 134−142

Supporting Information

Defects in Mouse Cortical Glutamate Uptake can be Unveiled in vivo by a Two-in-one Quantitative Microdialysis

Sandrine Parrot[1,*], Alex Corscadden[1], Louison Lallemant[2], Hélène Benyamine[2], Jean-Christophe Comte[1], Aline Huguet-Lachon[2], Geneviève Gourdon[2], Mário Gomes-Pereira[2]

[1]Inserm U1028; CNRS UMR5292; Université de Lyon; Lyon Neuroscience Research Center, Bron, F-69500, France

[2]Sorbonne Université, Inserm, Institut de Myologie, Centre de Recherche en Myologie, 75013 Paris, France

***Corresponding Author**
Sandrine PARROT, Inserm U1028, CNRS UMR5292, Université Claude Bernard Lyon 1, Centre Hospitalier Le Vinatier, Bâtiment 462 Neurocampus Michel Jouvet, 95 Bd Pinel, 69675 Bron Cedex, France.
Phone: +33 4 81 10 65 86. E-mail address: sandrine.parrot@univ-lyon1.fr

Table of contents

Glu uptake: methodological parameters to be considered

In the isotopic approach to challenge Glu uptake, we first tried to apply labelled Glu and mannitol at the same concentrations as previously used in rats, i.e., 1 mmol/L Glu solution (750 µmol/L of unlabeled Glu and 250 µmol/L ^{3}H-Glu), containing 120 µmol/L ^{14}C-mannitol. We failed to see any Glu loss in the hippocampus of 5 mice (data not shown), which led us to adapt the current protocol because tissue diffusion can differ according to animal species, age, brain area and physiopathology, as shown with various radiotracers or fluorescent macromolecules.[1] Besides, glutamate and mannitol diffusion in tissue also differs from each other, since glutamate enters cells by active transport, whereas mannitol can enter through unspecific carriers.[1, 2] Traditionally, probe recovery is below 20-25 %, or even lower when determined *in vitro* (5-10%), and above this order of magnitude, a higher value of recovery often reveals leaks at the level of the dialysis membrane (data not shown). A verification of the probe recovery in these 5 experiments showed that it was very similar between Glu and Man in each experiment. Glu and Man recovery was 14.2 ± 6.2 % and 14.6 ± 5.7 %, respectively (n=5), suggesting also a high variability from one experiment to another and the need to normalize the data, not only by comparing outlet concentrations to inlet concentrations of Glu and Man, as previously done, but by using Man as an internal standard, since Man is an exogenous compound that is removed from the extracellular space by unspecific carriers. Data were then expressed as ratios at the outlet corrected by the initial ratio in the inlet (Figure S1, next page). Figure S1 shows a slight trend of increase in the isotopic ratio at the end of the wash-out period. As it could reflect the subsequent release of compounds having infused the tissue, probably due to the administration of high concentrations.

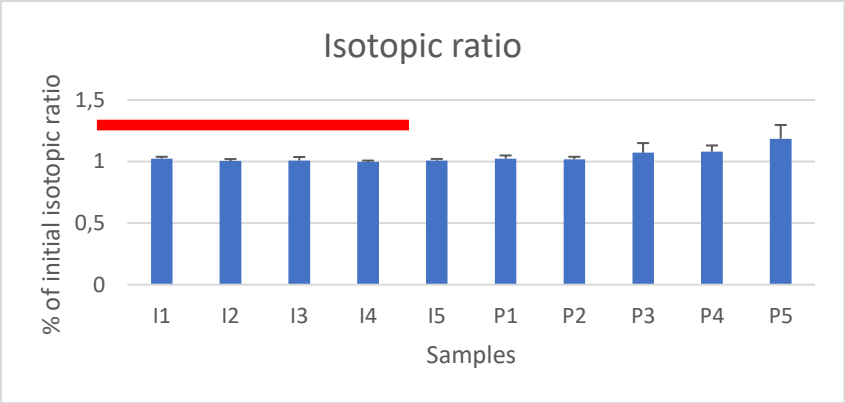

Figure S1. ***Isotopic ratio, as compared to the initial isotopic Glu/Man ratio determined in the hippocampus of five mice. Glu (750 µmol/L ^{1}H-Glu + 250 µmol/L ^{3}H Glu) and isotopic ^{14}C-Man 120 µmol/L were infused from I1 to I5 (red line).***

Then, we decided to lengthen the duration of collection and to lower the concentration of Glu in the isotopic infusion, mannitol was kept at a constant concentration (Figure S2).

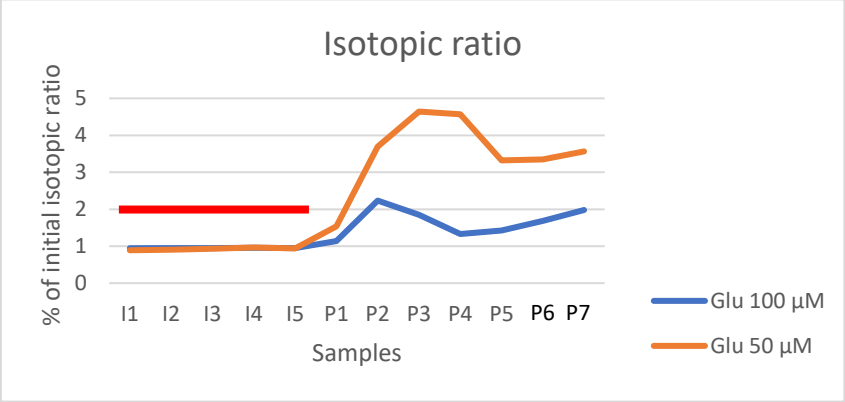

Figure S2. ***Example of the isotopic ratio between ^{3}H-Glu and isotopic ^{14}C-Man, as compared to the initial isotopic Glu/Man ratio determined in the hippocampus of five mice. Glu (50 µmol/L then 100 µmol/L ^{3}H Glu) and ^{14}C-Man 120 µmol/L were infused from I1 to I5 (red line). The perfusion of the 2nd solution with 100 µmol/L (orange plot) was separated by a 26-min wash-out from the 1st perfusion (blue plot).***

Figure S2 shows that the amplitude of the ratio during the wash-out is enhanced with 50 and 100 µmol/L labelled Glu administered in the same mouse. The two curves peak at 4-6 min after the end of isotopic infusion, which agrees with the kinetics observed in astrocyte cultures,[3] since 95% of glutamate clearance is ensured by an astrocytic carrier.[4] In these conditions our protocol can therefore reproduce *in vivo* the uploading of labelled Glu, as previously reported *in vitro*. We chose 100 µmol/L

as final concentration of labelled Glu for the rest of the study, in order to keep the concentration diffusing through the brain above the expected *in vivo* concentration (> 10 µmol/L).

Verification of probe placement

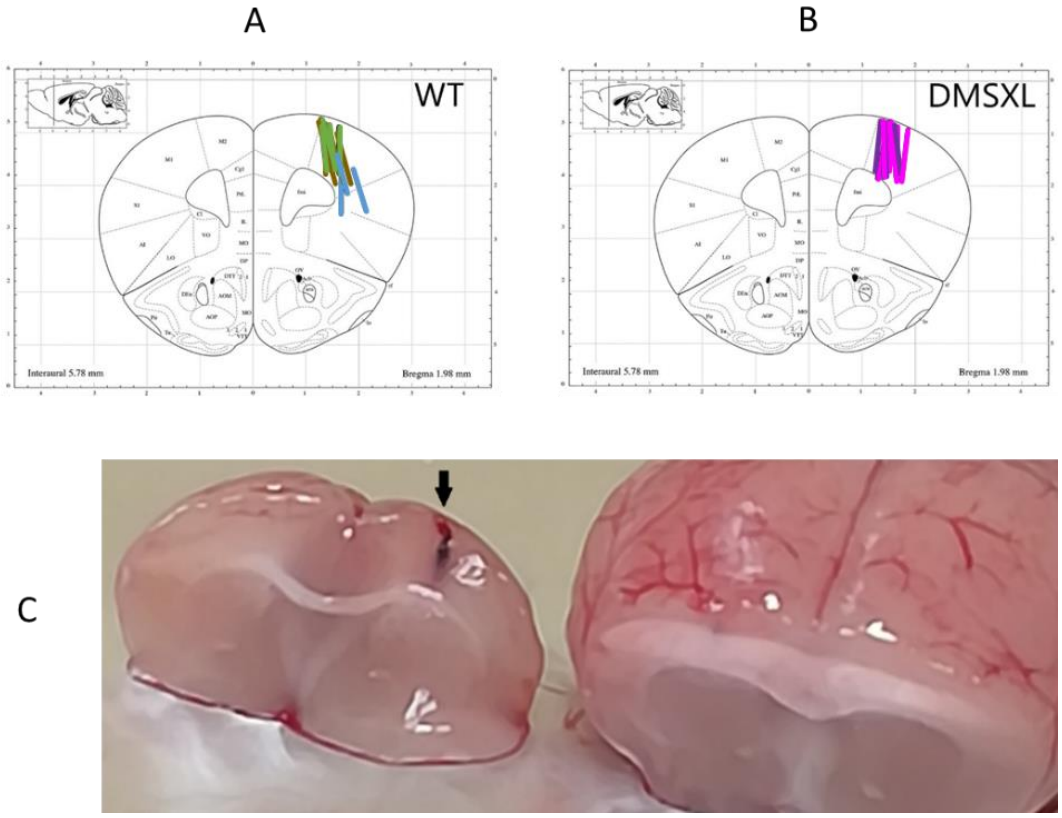

Figure S3. ***The verification of probe placement on the brains collected was done just after the experiment of radioactivity (A and B). The colored lines (A: green for WT, light blue for WT low, golden green for DHK WT; B: pink for DMSXL and purple for DHK DMSXL experiments) indicate the placement of the probes reported on the atlas by Franklin and Paxinos (reprinted with permission from Elsevier)[5], according to the blue track visible left by the microdialysis probe in the right motor cortex after brain cutting (C, indicated with a black arrow).***

Quantification of glutamine synthetase (GS; EC 6.3.1.2)

The enzyme converting glutamate to glutamine, named GLUtamate-ammonia Ligase (GLUL; EC 6.3.1.2; https://www.genecards.org/cgi-bin/carddisp.pl?gene=GLUL&keywords=GLUL), also known as glutamine synthetase (GS), was quantified using western blot (see Figure S4, next page).

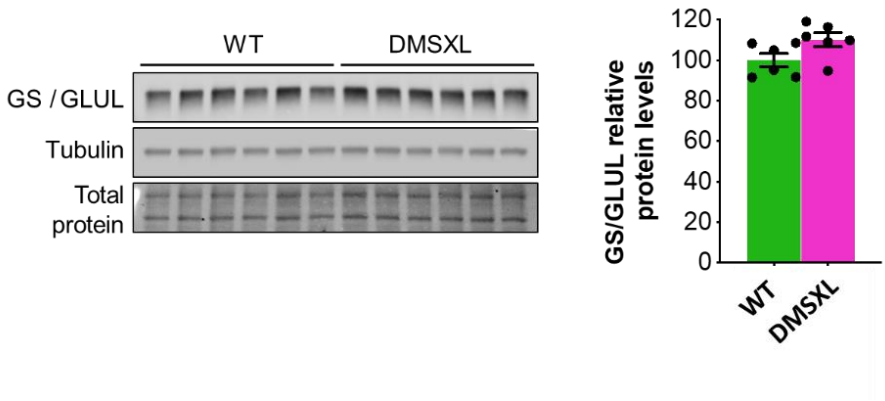

Figure S4. ***Left: Representative western blot detection of glutamine synthetase (GS/GLUL) and tubulin, as loading control, in mouse frontal cortex. Total protein levels are also shown. Right: Quantification of GS/GLUL steady state levels in the frontal cortex of 6 DMSXL and 6 WT mice at 2 months (right). Data are expressed as means (± SEM) relative to normalized WT values. No difference was observed between mouse groups (two-tailed Student's t-test).***

ZF fitting models: *in vivo* study

Four regression models have been previously reported in the literature to fit ZF data (Table S1, next page). Three of them are based on exponential equations: model #1 (Theory Fit) corresponds to the theoretical profile;[6, 7] model #2 (Simplified Fit; the correct equation could be read as $Y = Y_0 (1-\exp^{-kx})$ in [8]) can be used in most statistical software and model #3, based on a second-order polynomial curve and suitable for almost all curve profiles, has been used on human ZF data.[9]

Table S1. ***Models of regression proposed by the literature when using ZF microdialysis compared to our results on Glu extracellular concentrations***

Model ID	Model #1 (Theory Fit)	Model #2 (Simplified Fit)	Model #3 (used in ZF in humans)	Model #4 (Plateau fit)
References using the model	*6, 7*	*8, 10*	*9*	This study
Equation	$Y = Y_0 (1-\exp^{-k/X})$	$Y = Y_0 (1-\exp^{-kX})$	$Y = Y_0 + aX + bX^2$	$Y = (Y_0 - \text{Plateau}) \times \exp^{-KX} + \text{Plateau}$
Profile		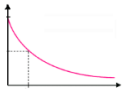	Not represented here	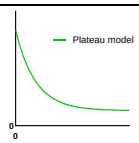
Quality of the model (a priori)	+++	++	+	Never challenged before
Our evaluation on our ZF data (a posteriori)	Poor fitting	Poor fitting	We did not use this model tailoring any curve and to be reserved rather for difficult-to-fit cases	Best fitting using a Plateau model

We followed the recommendations by K.C. Chen (2006) on small lengths of membrane and we considered the theoretical fitting curve, $C_{dial} = C_{ext} (1-e^{-MT \times A/FR})$, corresponding to an exponential decay equation based on 1/FR as the x-axis variable (C_{dial}, concentration in the dialysate; C_{ext}, true extracellular concentration in undisturbed tissue; MT, mass transfer coefficient; A, active area of the microdialysis probe membrane; FR, perfusion flow rate). The theory fitting to determine C_{ext} is believed to be more accurate than other fitting methods, which can misestimate true extracellular concentrations.[7] For that purpose, we were forced to model the equation in Matlab (scripts available as separate PDF files), with Y constraints to help converging to find values of C_{ext} at X=1/FR=0 (see Table S2, next page).

Table S2: ***R^2 values and Y0 values (C_{ext}) of the regression curve determined by zero flow method (theoretical fit, model #1) for cortical Glu, GABA and Asp levels in all mice (WT and DMSXL/DM genotypes)***

Theoretical model (#1)	Mouse	Glu	GABA	Asp	Theoretical model (#1)	Mouse	Glu	GABA	Asp
r2 (Matlab gives r)	DM 1	0,13	0,001	0,004	Y0 in µmol/L	DM 1	6,88	0,0055	0,074
	DM 2	0,86	0,61	0,79	LOD Glu = 0.003 µmol/L	DM 2	5,81	0,0075	0,16
	DM 3	0,70	0,40	0,63	LOD GABA = 0.0006 µmol/L	DM 3	3,76	0,0077	0,21
	DM 4	0,90	0,11	0,93	LOD Asp = 0.001 µmol/L	DM 4	2,12	0,0088	0,098
	DM 5	0,70	0,08	0,57		DM 5	5,48	0,0067	0,079
	DM 6	0,65	0,04	0,006		DM 6	0,099	0,0090	0,084
	Min	0,13	0,001	0,004		Min	0,099	0,0055	0,0739
	Max	0,90	0,61	0,93		Max	6,88	0,0090	0,2063
						Mean	4,02	0,0075	0,1166
						SD	2,55	0,0013	0,0539
	n	6	6	6		n	6	6	6

Theoretical model (#1)	Mouse	Glu	GABA	Asp	Theoretical model (#1)	Mouse	Glu	GABA	Asp
r2 (Matlab gives r)	WT 1	0,47	0,006	0,40	Y0 in µmol/L	WT 1	1,98	0,0043	0,095
	WT 2	0,89	0,33	0,79	LOD Glu = 0.003 µmol/L	WT 2	4,47	0,0085	0,11
	WT 3	0,68	0,002	0,008	LOD GABA = 0.0006 µmol/L	WT 3	0,17	0,0072	0,073
	WT 4	0,15	0,15	0,003	LOD Asp = 0.001 µmol/L	WT 4	2,67	0,0093	0,046
excluded (not converging)	WT 5				*excluded (not converging)*	WT 5			
	WT 6	0,92	0,001	0,54		WT 6	2,97	0,0046	0,098
	WT 7	0,62	0,021	0,16		WT 7	0,10	0,0084	0,090
	WT 8	0,30	0,43	0,008		WT 8	1,27	0,0087	0,086
	Min	0,15	0,001	0,003		Min	0,10	0,0043	0,046
	Max	0,92	0,43	0,79		Max	4,47	0,0093	0,11
						Mean	1,95	0,0073	0,086
						SD	1,58	0,0020	0,021
	n	7	7	7		n	7	7	7

In red font: data requiring to constrain the convergence of the regression to 10- or 100-fold less values

Probably due to our lack of data near x=0 µL/min, the goodness of the theoretical fittings was limited (Table S2, left), but C_{ext}, also named Y0, was estimated for all the mice, except for one that was excluded from the group (Table S2, right). Some authors have recommended to use ultra-low perfusion rates to achieve a better regression providing the shortest experimental time,[8] but in routine experiments, it seems to be rarely used due to long sampling constraints.[10]

Using the simplified model equation, $Y = Y_0 \exp^{-kX}$, we obtained a new set of r^2 values (Table S3, next page) and Y0 data (C_{ext}, shown in the main text of the manuscript Y0). We sometimes note a flattening of the curve near x = 0, likely due to the « by default » fitting constraints in Prism software (Figure S5, next page), but the data on r^2 values showed that model #2 had no significant impact on the goodness of the fitting as compared to the theoretical model (Table S3 vs Table S2). The model allowed to determine all the extracellular concentrations for GABA, Glu, and Asp (see the main text).

Table S3: ***R^2 values of the regression curve determined by zero flow method (simplified fit, model #2) for cortical Glu, GABA and Asp levels in all mice (WT and DMSXL/DM genotypes)***

Simplified model	Usual fit	Glu	GABA	Asp
r2	DM 1	0,85	0,43	0,75
	DM 2	0,72	0,21	0,53
	DM 3	0,78	0,22	0,58
	DM 4	0,67	0,75	0,76
	DM 5	0,64	0,09	0,40
	DM 6	0,77	0,03	0,05
	Min	0,64	0,03	0,05
	Max	0,85	0,75	0,76
	n	6	6	6
Simplified model	**Usual fit**	**Glu**	**GABA**	**Asp**
r2	WT 1	0,62	0,0004	0,61
	WT 2	0,83	0,47	0,78
	WT 3	0,66	0,65	0,19
	WT 4	0,53	0,01	0,01
excluded (outlier)	WT 5	*0,74*	*0,31*	*0,35*
	WT 6	0,88	0,03	0,66
	WT 7	0,74	0,13	0,42
	WT 8	0,63	0,63	0,21
	Min	0,53	0,0004	0,01
	Max	0,88	0,65	0,78
excluded (outlier)	n	7	7	7

However, the shape of our data is clearly different from an exponential growth equation (model #2). We observed a plateau of the decreasing curve at higher flow rates, which corresponds best to another model of exponential fitting, i.e., $Y = (Y_0 - \text{Plateau}) \times \exp^{-KX} + \text{Plateau}$.

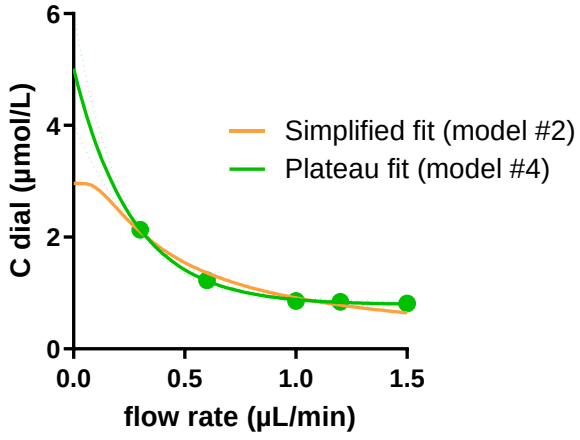

Figure S5: ***Example of a zero-flow experiment in mouse motor cortex. The principle is based on microdialysis dynamics according to the flow rate (FR) that modifies the probe recovery, and thereafter the dialysate concentration (C_{dial}). The concentration present in the extracellular space (C_{ext}) is supposed to be reached when FR = 0. An exponential plot of C_{dial} as a function of flow rate allows to determine C_{ext} with 5 different FR points (green circles). The simplified model (i.e., model #2) is obtained using an exponential curve (orange line, $Y = Y0\ (1-\exp^{-kX})$). However, a one-decay exponential curve provided the best fitting (green line +/-95% confidence interval, $Y = (Y0 - \text{Plateau}) \times \exp^{-KX} + \text{Plateau}$). Extracellular concentration is then extrapolated from the equation at null flow rate and the fitting with a plateau component allows to get higher values in C_{ext}.***

Data were reprocessed using this 4th model and r^2 data are given in Table S4 (this page), while the Y0 values are given in the main text of the manuscript. In this model, the values of fittings for Glu, GABA, and Asp levels were closer to 1 and much less dispersed than those obtained from theoretical model #1 and simplified model #2 (Figure S6, below).

If we consider the case of cortical GABA and Asp, the use of the Plateau Fit on our data led to improved regression coefficients, but also to more failure on regressions, with interrupted regressions analysis (7 out of 13 for GABA ; 3 out of 13 for Asp) or ambiguous values (3 out of 13 for Asp; 2 out of 13 for GABA), whereas the theoretical model never failed to determine C_{ext} for the three neurotransmitters (Table S4). To limit the failure of the regression, the introduction of a constraint on Y0 (<20 µmol/L) helped recover half of the ambiguous and interrupted calculations.

Table S4: *R^2 values of the regression curve determined by zero flow method (our fit with a plateau, model #4) for cortical Glu, GABA and Asp levels in all mice (WT and DMSXL/DM genotypes)*

r2	Plateau fit	Glu	GABA	Asp	Comparison of fits (Plateau vs Simplified) using F test (Reject of null hypothesis at p<0.05)
	DM 1	0,86	0,44	0,76	No difference for Glu and Asp ; comparison failure for GABA
	DM 2	0,90	0,37	0,66	Plateau fit as preferred model for Glu only (p=0.001), no difference for GABA and Asp
	DM 3	0,988	0,89	0,86	Plateau fit as preferred model (p=0.0003 for Glu; p=0.0006 for GABA) ; comparison failure for Asp
	DM 4	0,98	0,84	0,76	Plateau fit as preferred model for GABA only (p=0.0355), no difference for Glu and Asp
	DM 5	0,96	nd	0,63	Plateau fit as preferred model (p=0.0189 for Glu; p=0.0258 for Asp) ; comparison failure for GABA
	DM 6	0,97	failure	nd	Plateau fit as preferred model for Glu only (p<0.0001), comparison failure for GABA and Asp
	Min	0,86	0,37	0,63	
	Max	0,988	0,89	0,86	
	n	6	4	5	
r2	Plateau fit	Glu	GABA	Asp	Comparison of fits (Plateau vs Simplified) using F test (Reject of null hypothesis at p<0.05)
	WT 1	0,92	0,14	0,90	Plateau fit as preferred model (p<0.0001 for Glu; p<0.0001 for Asp); no difference for Asp)
	WT 2	0,993	0,82	0,93	Plateau fit as preferred model (p<0.0001 for Glu; p=0.0151 for GABA; p=0.0002 for Asp)
	WT 3	0,86	0,61	nd	Plateau fit as preferred model for Glu only (p=0.0011), comparison failure for GABA and Asp
	WT 4	0,83	nd	nd	Plateau fit as preferred model for Glu only (p=0.001), comparison failure for GABA and Asp
excluded (outlier)	WT 5	*0,97*	*nd*	*0,70*	not done
	WT 6	0,989	failure	0,92	Plateau fit as preferred model (p<0.0001 for Glu and Asp) ; comparison failure for GABA
	WT 7	0,98	nd	0,92	Plateau fit as preferred model for Glu only (p<0.0001), no difference for Asp ; comparison failure for GABA
	WT 8	0,90	0,93	0,60	Plateau fit as preferred model (p=0.0001 for Glu; p<0.0001 for GABA; p=0.0228 for Asp)
	Min	0,83	0,14	0,60	
	Max	0,993	0,93	0,93	
	n	7	4	5	

red, ambiguous regressions	*ambiguous values* i.e., despite missing data on replicates, Prism software found a converging value at x=0 (a set of data was excluded due to its aberrant ZF profile)
blue, interrupted regressions	not done (nd) i.e., Prism software failed to find a converging value at x=0 (missing data on replicates or atypical profiles of the curves)
In yellow, 2nd regressions after	introducing a constraint to force convergence to a Y0 value inferior to 20 µmol/L in Prism Software

The observation of some failures of fitting with our Plateau model was not seen in another brain structure, the hippocampus, in which the number of failed regressions was null with the simplified model, or below 3 out of 29 using our 'decay with plateau' fitting (not shown). The homogeneity of neurotransmitter localization, rather than the homogeneity of neuronal tissue, might explain such a discrepancy. However, in every case of failure of our Plateau fit model to determine extracellular levels in both brain areas tested, GABA and Asp (but rarely Glu) were found at very low concentrations (Figure S6, page 12). These results suggest that our Plateau fitting model for cortical Glu might exhibit limits to estimate the poor bioavailability of GABA and Asp, as compared to Glu, especially in the cortex. Regression models are known to be very sensitive to any variability; and the variabilities generated when sampling, storing, and the analysis by CE-LIFD must have affected the samples with lower concentrations of compounds.

Lastly, to verify the statistical validity of our Plateau Fit, a comparison of Simplified usual model (#2) and Plateau model (#4) regressions using the extra-sum-of-squares F test was performed. The analysis was performed on the 34 concentrations of Glu, GABA, Asp determined by both models: the fit was judged ambiguous for 3 values of GABA for both models; the fit with model #4 was preferred for 20 values of Glu, GABA and Asp concentrations; no difference was found between models #2 and #4 for 11 values of Glu, GABA, and Asp concentrations. Even if a higher value of r^2 does not necessarily imply a better fitting in a regression analysis, the results of our F test, comparing the improvement of sum-of-squares with a more complicated model (here, Plateau Fit, model #4 compared to Simplified Fit, model #2) vs. the loss of degrees of freedom induced by model #4 exhibiting more parameters, clearly showed that the fit obtained with model #2 was never preferred, while the fit with obtained model #4 was statistically preferable twice as often. Taking together, these results are in favor of the use of a more complicated regression model when fitting unusual ZF data, as we found for neurotransmitter amino acids.

Besides, as illustrated in our example in Figure S5, the simplified usual curve (model #2) gave a value of C_{ext} equal to 2.96 µmol/L for Glu, whereas the plateau fit (model #4) determined C_{ext} at 5.02 µmol/L, i.e., a two-fold increase in concentration relative to the first model in this peculiar ZF experiment. Table S5 shows the differences of the 95% confidence intervals for two models (Simplified vs Plateau fits) from extracellular GLU of the 7 WT mice. Those results suggest that, despite the absence of overlapping for two mice and the wider intervals using the Plateau fit for the remaining six mice, the individual estimations, and thus, the estimations of the means per group, are still both in the range of the results obtained by other sampling approaches.[11-13]

Table S5: ***95% confidence intervals for Y0 values (C_{ext}) of the regression curve determined by zero flow method for cortical Glu levels in 8 WT mice***

Mouse	Simplified fit (model #2)	Plateau fit (model #4)	Interval overlapping
WT 1	1.592 to 2.474	0.5254 to 11.50	Yes
WT 2	3.434 to 5.040	6.631 to 9.398	No
WT 3	0.6997 to 1.384	-1.313 to 8.135	Yes
WT 4	2.190 to 3.552	-5.596 to 23.84	Yes
WT 5	2.095 to 2.908	Wide	Yes (data excluded)
WT 6	2.239 to 3.681	4.025 to 6.009	No
WT 7	1.227 to 1.706	2.262 to 5.030	Yes
WT 8	1.077 to 1.470	0.8345 to 4.616	Yes

Figure S6. ***A- Number of failures/successes when performing the plateau fit in ZF experiments per neurotransmitter. B- Amino acid concentrations estimated with the usual fit in regard of the success or failure of ZF method using the plateau fit (merged data, *p<0.05, Two-way ANOVA with Failure/success Factor as significant ($F_{2,36}$=4.89) and neurotransmitter Factor as not significant, no interaction). C, D &E-. Amino acid concentrations estimated with the usual fit in regard of the success or failure of ZF method using the plateau fit (data range per neurotransmitter, means indicated***

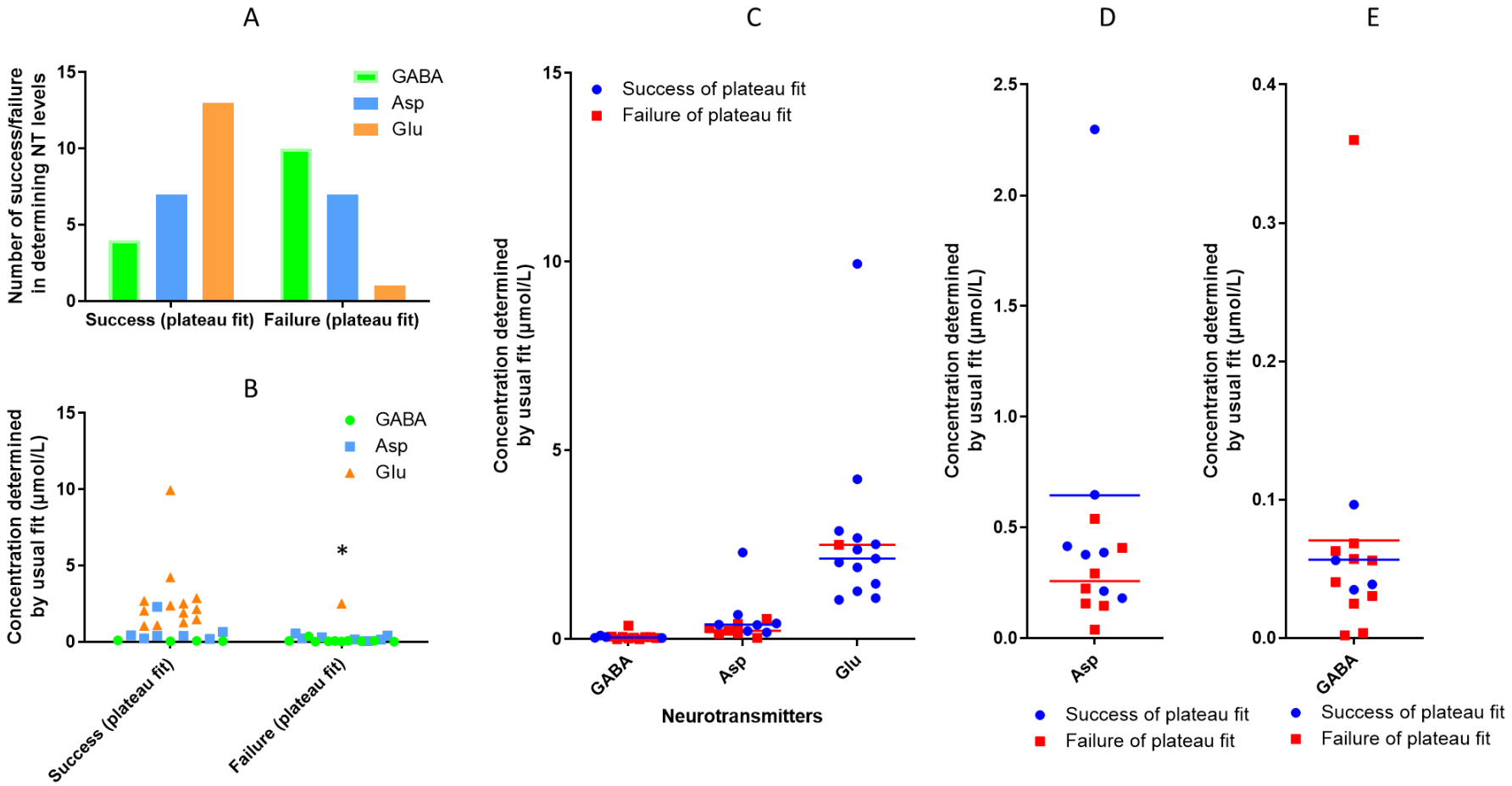

ZF fitting models: in vitro study

In order to assess if the introduction of a plateau in a one-decay curve improved the fitting for *in vivo* Glu, we mimicked *in vitro* a ZF experiment with labeled and unlabeled Glu. The data obtained with models #1 (theory), #2 (simplified, usual) and #4 (plateau) are given in Figure S7.

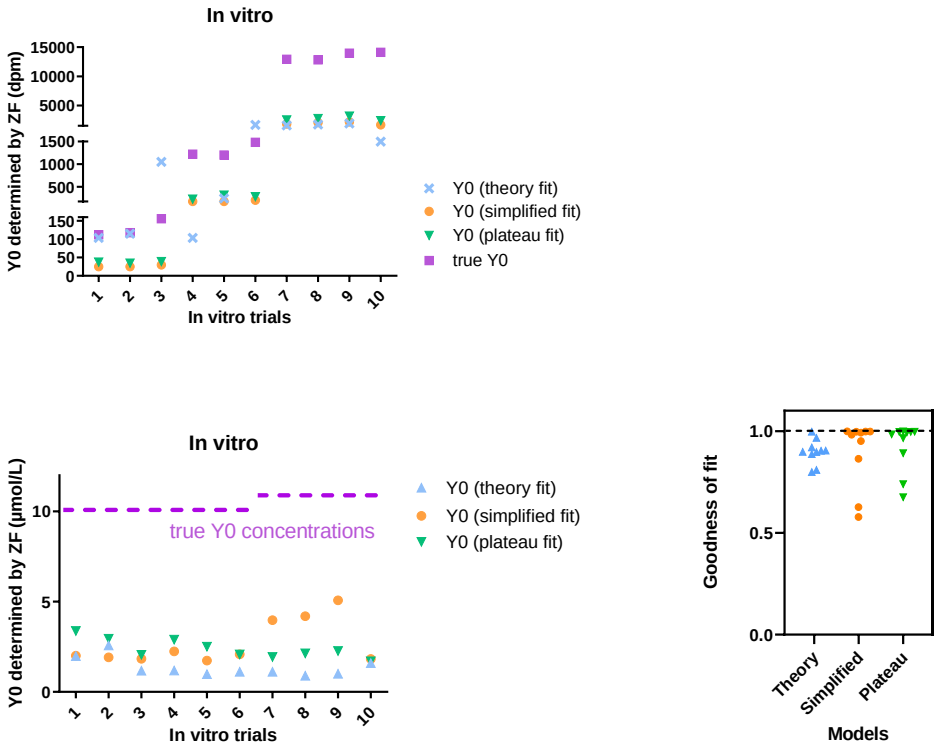

Figure S7. ***Zero flow method carried out in vitro in a 10 µM Glu solution containing ^{3}H-Glu (0.1, 1 or 10 µM, 3 or 4 assays per concentrations, n=10 in total). Top: Determinations of Y0 using dpm. Bottom: Determinations of Y0 using sample concentrations (left) and goodness of the regressions (n=10) (right).***
Theory fit = Model #1; Simplified (usual) fit = Model #2; Plateau fit = Model #4.

In contrast to the *in vivo* studies, R^2 values were rather similar whatever the fitting model chosen, suggesting that the dispersions of the goodness values found in vivo do not depend on the poor quality of sampling, nor models to fit ZF data, but on the extracellular matrix. When considering our data on Y0 values, we found that the extracellular concentrations of Glu were globally similar whatever the fitting model, but they all failed to estimate the true concentration, even the theoretical model. The Plateau fit yielded more often the nearest true value of Y0, with less variability. Our *in vitro* results clearly show that model #4 is a relevant alternative to models #1 and #2 to reach precise true extracellular concentrations despite a lack of accuracy we observed whatever the model used. Taking together both in vivo and in vitro statistical analysis on ZF data presented in this Supporting

Information, we can conclude that model #4 introducing a plateau in the nonlinear regression equation does not fit better and in a more reproductive manner per se, but fits better ZF neurotransmitter amino acids because it takes into account the more complicated profile of ZF data found in vivo. In particular, the additional parameter, namely the plateau, introduced in the regression equation, allows to fit both in vitro and in vivo profiles since the value of the plateau starts from zero. This peculiar ZF profile found on in vivo ZF data from neurotransmitter amino acid sampling is certainly linked to their specific physiological regulations and/or bioavailabilities in mouse frontal cortex as further discussed in the main text of the manuscript.

List of MATLAB scripts

The main script and its three associated scripts are available as Supporting information: cn1c00634_si_002.pdf, cn1c00634_si_003.pdf, cn1c00634_si_004.pdf, cn1c00634_si_005.pdf, respectively.

References

[1] Sykova, E., and Nicholson, C. (2008) Diffusion in brain extracellular space, *Physiological reviews 88*, 1277-1340.

[2] Bruhn, T., Christensen, T., and Diemer, N. H. (1995) Microdialysis as a tool for in vivo investigation of glutamate transport capacity in rat brain, *Journal of neuroscience methods 59*, 169-174.

[3] Parpura, V., Liu, F., Brethorst, S., Jeftinija, K., Jeftinija, S., and Haydon, P. G. (1995) Alpha-latrotoxin stimulates glutamate release from cortical astrocytes in cell culture, *FEBS letters 360*, 266-270.

[4] Danbolt, N. C., Furness, D. N., and Zhou, Y. (2016) Neuronal vs glial glutamate uptake: Resolving the conundrum, *Neurochemistry international 98*, 29-45.

[5] Franklin, K., and Paxinos, G. (2001) The Mouse Brain in Streotaxic Coordinates: Academic Press.

[6] Jacobson, I., Sandberg, M., and Hamberger, A. (1985) Mass transfer in brain dialysis devices--a new method for the estimation of extracellular amino acids concentration, *Journal of neuroscience methods 15*, 263-268.

[7] Chen, K. C. (2006) Validity of intracerebral microdialysis, In *Handbook of Microdialysis Methods, Applications and Perspectives* (Westerink, B. H. C., and Cremers, T. I. F. H., Eds.), pp 47-70.

[8] Menacherry, S., Hubert, W., and Justice, J. B., Jr. (1992) In vivo calibration of microdialysis probes for exogenous compounds, *Analytical chemistry 64*, 577-583.

[9] Cavus, I., Widi, G. A., Duckrow, R. B., Zaveri, H., Kennard, J. T., Krystal, J., and Spencer, D. D. (2016) 50 Hz hippocampal stimulation in refractory epilepsy: Higher level of basal glutamate predicts greater release of glutamate, *Epilepsia 57*, 288-297.

[10] Ulrich, J. D., Burchett, J. M., Restivo, J. L., Schuler, D. R., Verghese, P. B., Mahan, T. E., Landreth, G. E., Castellano, J. M., Jiang, H., Cirrito, J. R., and Holtzman, D. M. (2013) In vivo measurement of apolipoprotein E from the brain interstitial fluid using microdialysis, *Molecular neurodegeneration 8*, 13.

[11] Alexander, G. M., Deitch, J. S., Seeburger, J. L., Del Valle, L., and Heiman-Patterson, T. D. (2000) Elevated cortical extracellular fluid glutamate in transgenic mice expressing human mutant (G93A) Cu/Zn superoxide dismutase, *Journal of neurochemistry 74*, 1666-1673.

[12] Lv, Y., Dai, W., Ge, A., Fan, Y., Hu, G., and Zeng, Y. (2018) Aquaporin-4 knockout mice exhibit increased hypnotic susceptibility to ketamine, *Brain and behavior 8*, e00990.

[13] Hascup, K. N., Hascup, E. R., Pomerleau, F., Huettl, P., and Gerhardt, G. A. (2008) Second-by-second measures of L-glutamate in the prefrontal cortex and striatum of freely moving mice, *The Journal of pharmacology and experimental therapeutics 324*, 725-731.